Belief Shocks and Implications of Expectations about Growth-at-Risk*

Maximilian BOECK[1] and Michael PFARRHOFER[2]

[1] *Friedrich-Alexander-University Erlangen-Nuremberg*
[2] *Vienna University of Economics and Business*

This paper revisits the question of how shocks to expectations of market participants can cause business cycle fluctuations. We use a vector autoregression to estimate dynamic causal effects of belief shocks which are extracted from nowcast errors about output growth. In a first step, we replicate and corroborate the findings of Enders *et al.* (2021). The second step computes nowcast errors about growth-at-risk at various quantiles. This involves both recovering the quantiles of the nowcast distribution of output growth from the Survey of Professional Forecasters; and, since the true quantiles of output growth are unobserved, estimating them with quantile regressions. We document a lack of distinct patterns in response to shocks arising from nowcasts misjudging macroeconomic risk. Although the differences are statistically insignificant, belief shocks about downside risk seem to produce somewhat sharper business cycle fluctuations.

JEL: C22, C32, E32, E71
Keywords: Tail risk, density forecasting, nowcast, quantile regression

* *Contact*: Maximilian Boeck, School of Business, Economics and Society, Friedrich-Alexander-University Erlangen-Nuremberg. E-mail: maximilian.boeck@fau.de. We thank Zeno Enders for useful suggestions and comments. Pfarrhofer gratefully acknowledges financial support by the Jubiläumsfonds of the Oesterreichische Nationalbank (OeNB, project 18765).

1. INTRODUCTION

This paper revisits the question of how shocks to expectations of market participants can cause business cycle fluctuations (see, e.g., Beaudry and Portier, 2006; 2014). We build upon the empirical framework of Enders *et al.* (2021) who discuss the identification of belief shocks. Usually, *expectations* about variables enter theoretical models as expected values conditional on some information set. In empirical models, they are often operationalized as mean-based predictions. That is, they are summary statistics of predictive distributions. This potentially disregards higher-order moments and abstracts from implied judgements of economic agents about macroeconomic risks.[1]

We diverge partly from the related literature and explicitly leverage full predictive distributions. Our first contribution is to replicate the findings of Enders *et al.* (2021), which are based on using the median consensus nowcast for US real gross domestic product (GDP) growth from the Survey of Professional Forecasters (SPF). They use this data to compute nowcast errors (NEs, defined as the difference between realized output growth and nowcasts). Their identification scheme then discriminates between belief and non-belief shocks via sign restrictions in a vector autoregression (VAR). They impose the belief shock to induce negative co-movement between output and NEs, while the non-belief shocks cause positive co-movement. This reflects the notion that a favorable belief shock (e.g., an overly optimistic outlook due to noisy signals observed by markets) shifts predictions beyond actual growth. This results in a negative NE while increasing output growth.

The second contribution is to move beyond the point prediction and recover the probabilistic distribution of nowcasted output growth in the US. This aspect of our work is motivated by the recent interest in macroeconomic (tail) risk due to the influential paper by Adrian *et al.* (2019). A common definition of macroeconomic risk is to consider the conditional quantiles of some underlying series of interest. The quantiles of output growth, for instance, are referred to as growth-at-risk (GaR) at some pre-defined probability. Related work finds time-varying macroeconomic risk to be at least partly predictable (see, e.g., Adams *et al.*, 2021; Clark *et al.*, 2023).

Evaluating and processing nowcasts of tail risk comes with two main challenges. First, the SPF does not contain probabilistic predictions in a format required for our analysis. Our solution is to rely on the ensemble methods proposed by Krüger and Nolte (2016) to recover the implied predictive distribution from individual point forecasts of SPF participants. Second, the quantiles of the dynamic process governing output growth are not observed. Here, we rely on time-varying parameter quantile

[1] The literature investigating belief distortions/wedges or disagreement usually focuses on mean outcomes and the cross-sectional dispersion of beliefs or expectations (Lahiri and Sheng, 2010; Dovern *et al.*, 2012; Adam *et al.*, 2021; Bianchi *et al.*, 2022; Bhandari *et al.*, 2022; Boeck, 2023; Born *et al.*, 2023; Pei, 2024).

regression (TVP-QR, see e.g., Pfarrhofer, 2022) to estimate the real-time quantiles of output growth (see Loria *et al.*, 2024, for a related approach). These two ingredients are used to compute reduced form GaR-NEs (which measure an inaccurate assessment of potential best/worst-case scenarios about the economic outlook; in this context, see e.g., the Federal Reserve Bank of New York Outlook-at-Risk dashboard), which we then employ to study the dynamic effects of belief shocks.

Our empirical results can be summarized as follows. First, we demonstrate the replicability of the results of Enders *et al.* (2021) in a narrow sense. Replicability in this context refers to extending the sampling period and considering alternative specifications in addition to the original implementations. Second, in a wide sense, we investigate whether belief shocks about GaR induce distinct business cycle fluctuations. The answer to this question is no. Indeed, we find very similarly shaped responses. This is true both when comparing our quantile-based estimates to the original framework, but also, when we compare, e.g., downside to upside risk. We conjecture that this is because the nowcast distribution of output growth, which we recover from the SPF, turns out to be rather symmetric for most of the sample. This relates to the nowcast (rather than forecast) setting, where the latter is usually the focus of studies about macroeconomic risk. Although the differences are statistically insignificant, belief shocks about downside risk seem to produce somewhat sharper business cycle fluctuations.

The paper proceeds as follows. In Section 2 we describe the SPF data, the original framework to extract belief shocks, and our extensions to recovering a suitable probabilistic predictive distribution. Section 3 discusses the VAR framework and identification procedure for belief shocks, before moving on to our main empirical results. Section 4 concludes.

2. SURVEY- AND NOWCAST DISTRIBUTIONS

2.1. *The Survey of Professional Forecasters*

Predictions about the current state of the economy lie at the heart of our paper. The SPF is a quarterly survey of such macroeconomic predictions, maintained by the *Federal Reserve Bank of Philadelphia*. It collects projections, from a changing panel of participants, which are submitted in form of a single number which is the point forecast of the target variable by the respective forecaster. For many applications, it is sufficient to aggregate these by computing the mean or median consensus prediction at any given point in time for any desired forecast horizon. This produces a sequence of (point) forecasts and yields a single time series based on an equal-weighted combination. Indeed, this is the default format for downloading SPF data, and what Enders *et al.* (2021) use in their original paper.

In our paper, as an extension, we intend to identify belief shocks related to the full predictive distribution. They are extracted from NEs about GaR. While the SPF in principle collects probabilistic forecasts, these come in the form of probability bins for a specific horizon and transformation of output, which we thus cannot use for our purposes. For this reason, we recover nowcast distributions from point predictions of individual forecasters as follows. Suppose that the predictive density $y_t^{(f,i)}$ of forecaster i at time t has mean μ_{it} and variance ς_{it}^2. We observe the point prediction μ_{it} (made at time t, when realizations were not yet available because GDP is released with a lag) of individual forecaster $i = 1, \ldots, N_t$, but we do not observe the variance ς_{it}^2.

Due to the design of the SPF, with coverage and number of forecasters N_t varying over time, we aim to construct an ensemble forecast using participants that are exchangeable. Define the average mean forecast $\overline{\mu}_t = N_t^{-1} \sum_{i=1}^{N_t} \mu_{it}$ and forecaster disagreement $s_t^2 = (N_t - 1)^{-1} \sum_{i=1}^{N_t} (\mu_{it} - \overline{\mu}_t)^2$ as the cross-sectional mean and variance of the point predictions across all survey forecasts. What is missing here is the unpredictable randomness (encoded in ς_{it}^2) of the target series surrounding the nowcasts. To solve this issue, we follow Krüger and Nolte (2016) and use an ensemble method, which has been shown to work well for the SPF.

In particular, we assume that the ensemble nowcast distribution $y_t^{(f)}$ can be written as an equal-weighted mixture of Gaussians with a common (but unknown) variance:

$$y_t^{(f)} = \frac{1}{N_t} \sum_{i=1}^{N_t} \mathcal{N}\left(\mu_{it}, \varsigma^2\right), \tag{1}$$

where ς^2 is the sole parameter to be estimated. Note that this implies that the joint forecast distribution $y_t^{(f)}$ has a mean equal to the average across forecasters, $\overline{\mu}_t$, and its variance is given by $\overline{\varsigma}_t^2 = s_t^2 + \varsigma^2$. The first variance component measures dispersion over the cross-section of forecasters, while the second reflects the unpredictable part of GDP. Note that even though the individual components in the sum of Eq. (1) are Gaussian, the mixture allows for nowcast distributions with highly non-Gaussian features such as skewness, multi-modality or heavier-than-normal tails (see, e.g., Frühwirth-Schnatter, 2006, for a detailed discussion). Estimates for ς^2 are obtained from a rolling window of $\tau = 12$ quarters, i.e., three years worth of quarterly nowcasts. We optimize the parameter using the continuous ranked probability score (CRPS) as predictive loss that we seek to minimize for the pool of forecasters.[2]

[2] The CRPS $(f(\bullet|\boldsymbol{\theta}), w) = \int_{-\infty}^{\infty} (F(z|\boldsymbol{\theta}) - \mathbb{I}(w \leq z))^2 \, \mathrm{d}z$, where $f(\bullet|\boldsymbol{\theta})$ refers to the probability density function of some distribution with parameter vector $\boldsymbol{\theta}$, $F(z|\boldsymbol{\theta}) = \int_{-\infty}^{z} f(\mathfrak{w}|\boldsymbol{\theta}) \mathrm{d}\mathfrak{w}$ is the corresponding cumulative distribution function, and w is the realized value. In our application, $f(\bullet|\boldsymbol{\theta})$ is a Gaussian such that $\boldsymbol{\theta}$ comprises a known mean and unknown variance. See Gneiting and Ranjan (2011) for details and a discussion of the favorable properties of the CRPS as a scoring rule.

It remains to explicitly define the minimization problem. We use $y_t^{(r)}$ to denote the real-time realization of GDP growth and assume normally distributed nowcasts, in line with Eq. (1): $\hat{\varsigma}_\tau^2 = \min_{\varsigma^2} \left(\sum_{t=(\tau-w)}^{\tau-1} \sum_{i=1}^{N_t} \text{CRPS} \left(\mathcal{N}(\mu_{it}, \varsigma^2), y_t^{(r)} \right) \right)$. Moving the rolling window forward yields a sequence of estimates $\hat{\varsigma}_t^2$. Two features are worth mentioning. First, this introduces time-varying variances, as we have estimates for each t, and w governs the persistence of these estimates. Second, even though the $\hat{\varsigma}_t^2$'s are dated at time t, we only use information up to $t-1$ (i.e., we do not mix information sets). We may use this procedure to obtain Monte Carlo samples or quantiles from the ensemble predictive distribution in Eq. (1):

$$\frac{1}{N_t} \sum_{i=1}^{N_t} \mathcal{N}(\mu_{it}, \hat{\varsigma}_t^2). \tag{2}$$

Indeed, this is how we obtain the full predictive distribution of the SPF ensemble nowcast whose pth quantile, $y_{pt}^{(f)}$, is the ensemble nowcast for GaR at quantile p at time t. The consensus nowcast is given by $\overline{y}_t^{(f)} = \overline{\mu}_t$.

2.2. *Estimating real-time quantiles of output growth*

The final challenge is that the *true* quantiles of output growth are not observed. Each observation of GDP is just a single realization of an underlying stochastic process, and comparing these realizations to our GaR expectations is futile. Next, we thus discuss how we estimate the real-time latent quantiles of the GDP growth process, which we require to compute NEs quantile-by-quantile (by contrast, having access to explicit measures of quantiles is not necessary when the focus is on out-of-sample predictive inference and designing scoring rules used for model selection, see, e.g., Gneiting and Ranjan, 2011).

Our baseline framework is similar to Loria *et al.* (2024); i.e., to estimate the unobserved quantiles of output, we use a variant of quantile regression. In particular, given its substantial degree of flexibility, our implementation is based on a Bayesian time-varying parameter quantile regression (TVP-QR) as in Pfarrhofer (2022). Let $\{y_t\}_{t=1}^T$ denote a scalar dependent variable, $\{\boldsymbol{x}_t\}_{t=1}^T$ comprises K predictors at time $t = 1, \ldots, T$, and $q_p(\boldsymbol{x}_t) = \boldsymbol{x}_t' \boldsymbol{\beta}_{pt}$ is the pth quantile function of y_t given $\boldsymbol{x}_t$ for $p \in (0, 1)$. We use a model of the form $y_t = \boldsymbol{x}_t' \boldsymbol{\beta}_{pt} + \varepsilon_t$ with $\int_{-\infty}^0 f_p(\varepsilon_t) d\varepsilon_t = p$, i.e., the pth quantile of the error distribution $f(\bullet)$ is equal to zero. Specifically, we assume ε_t to follow an asymmetric Laplace (AL) distribution with scale σ_p^2. The $\boldsymbol{\beta}_{pt}$'s are quantile-specific vectors of size $K \times 1$ which collect the parameters that vary over time. We assume an independent random walk state equation for each of these parameters and rely on a dynamic shrinkage prior for regularization.

This framework consists of two crucial ingredients. First, it allows coefficients to vary at quantile p, allowing for heterogeneous effects across specific parts of the distribution of y_t. Second, the magnitudes of these effects are allowed to vary over time. The former reflects the literature on measuring tail risks of GDP growth, following Adrian *et al.* (2019), while the latter allows for another layer of nonlinearity that has been found to improve accuracy (see, e.g., the corresponding discussion in Clark *et al.*, 2024). The target variable y_t is the respective first released vintage of the annualized growth rate of real GDP. This data is from the *Real-Time Data Set for Macroeconomists*. We choose these vintages such that our target variable is as close as possible to the conceptual variable that the participants of the SPF were asked to forecast at the time.

Our vector of predictors contains Q common factors $\boldsymbol{f}_t$ that drive economic fluctuations in the US economy. In particular, we use a macroeconomic real-time dataset of 80 variables such that it resembles the potential information set a forecaster of the SPF has access to.[3] We extract extract $Q = 4$ factors following Stock and Watson (2002). Additionally, we add lags of the National Financial Conditions Index (NFCI), labeled z_t, which has been identified as an important variable that shifts the quantiles of GDP, lags of the dependent variable and an intercept term. We use $P = 4$ lags such that $\boldsymbol{x}_t = (1, y_{t-1}, \ldots, y_{t-P}, z_{t-1}, \ldots, z_{t-P}, \boldsymbol{f}'_{t-1}, \ldots, \boldsymbol{f}'_{t-P})'$.

Running our algorithm produces estimates for the quantiles of GDP growth for each point in time, i.e., the fitted "realized" values $\hat{y}^{(r)}_{pt} = \boldsymbol{x}'_t \boldsymbol{\beta}_{pt}$, which we interpret as the best possible estimate of the *true real-time* quantile (we stress that these quantiles are subject to potential measurement errors, and some of our results below thus must be interpreted with caution). Note that our procedure is based on an expanding window of observations, such that the information sets of the quantile model and the one available to the SPF forecasters is consistent. Our implementation is fully Bayesian, which implies that we obtain a posterior distribution for the fitted quantiles. We summarize this distribution by taking the posterior median at a particular quantile of interest.

2.3. *Empirical estimates for growth-at-risk nowcast errors*

Our full sample runs from 1968Q4 to 2019Q4. Figure 1 shows real GDP growth and the quantiles estimated with TVP-QR in the upper panel. The shaded areas range between the 10th and 90th percentiles. The solid line is actual GDP growth, while the dashed line indicates the 50th percentile estimated using TVP-QR. The lower panel is a chart of the SPF nowcast distribution. The shaded area again reflects the 80 percent credible set, "Median" indicates the default SPF aggregation as used

[3] The dataset is described in more detail in the Appendix B. Our results are robust to relying on the most recent data vintage of the FRED-QD database. In this case, we explicitly exploit the most recently available information to measure the quantiles of the first release vintage of GDP for each period.

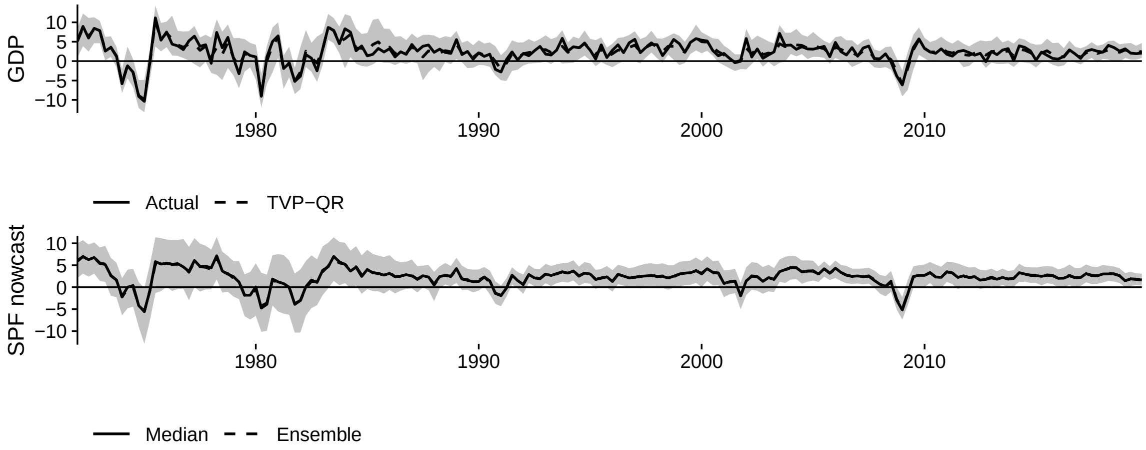

Fig. 1: Real GDP growth, estimated quantiles and SPF nowcast distribution. Shaded areas show the 10th and 90th percentiles around the median; "Median" refers to the default SPF.

in Enders *et al.* (2021) whereas "Ensemble" is the point nowcast arising from using the methods of Krüger and Nolte (2016) as described above. These two approaches coincide for the mean/median, but our implementation yields a full predictive distribution.

Next, we formally define the versions of NEs that we consider descriptively and in our structural application. We previously denoted the consensus nowcast with $y_t^{(f)}$ and the realization as $y_t^{(r)}$. These serve as the basis for the variant that replicates Enders *et al.* (2021). Recall that our estimates from TVP-QR yield the quantile-based counterpart for observed GDP, $\hat{y}_{pt}^{(r)}$, and that the quantiles of the distribution in Eq. (2) define our SPF nowcast of the pth quantile, $y_{pt}^{(f)}$. The NEs are:

$$\mathrm{ne}_t = y_t^{(r)} - \overline{y}_t^{(f)}, \tag{3}$$

$$\mathrm{ne}_{pt} = \hat{y}_{pt}^{(r)} - y_{pt}^{(f)}. \tag{4}$$

We purge the NEs of any remaining predictable components by running ARIMA models with automatic lag selection.[4] Figure 2 shows the resulting NEs; "Actual" refers to those for the consensus nowcast and actual GDP observations, as in Eq. (3), while the colored lines mark those for GaR at the indicated quantile based on Eq. (4). The baseline NEs are identical (up to a scaling factor) to those shown in Figure 1 of Enders *et al.* (2021). The dynamics of our quantile-based versions are similar. Indeed, all our versions of NEs are positively correlated at varying strengths (additional results are provided in the Online Appendix). For the median, the correlation exceeds 0.8 and we conclude that our framework to extract quantile-based nowcast errors yields reasonable results.

[4] For some quantiles the NEs exhibit a modest amount of persistence, which we eliminate with this procedure. We also estimated the VAR model in Section 3 without purging the NEs from predictable components. In this case, the main results for output are very similar, but there is some persistence in the responses of the nowcast errors.

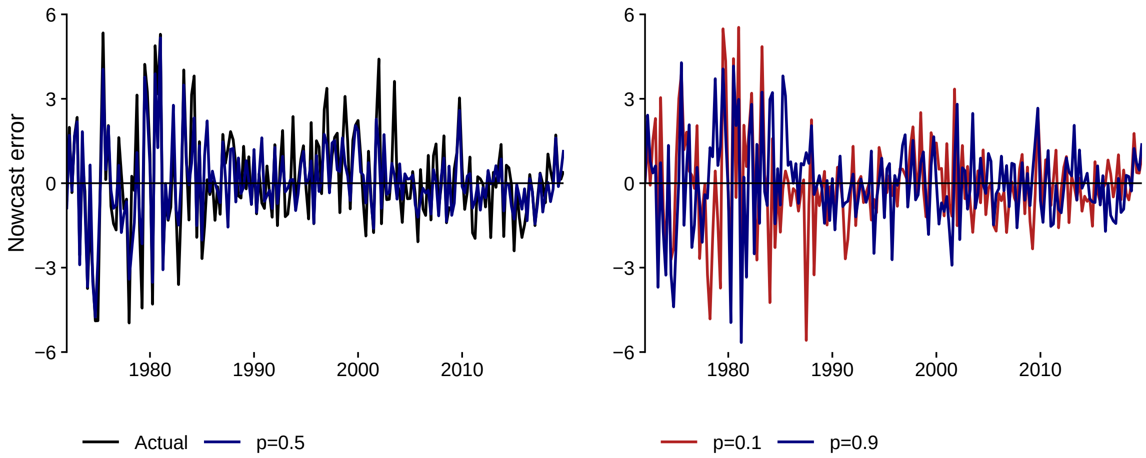

Fig. 2: NEs computed with actual realizations of real GDP growth and the indicated selected GaR probabilities.

3. BELIEF SHOCKS AND THEIR EFFECTS ON THE BUSINESS CYCLE

We now turn to the specification and identification of the structural VAR that we use to recover dynamic causal effects of belief shocks. This section contains the main empirical results: those for our narrow replication of the original implementation and our extension focusing on nowcasts about GaR.

3.1. *The vector autoregression and identification*

As laid out in Enders *et al.* (2021), belief shocks can be extracted from the NE. We use a bivariate VAR that features the NE (ne_t for the plain version, and ne_{pt} when we consider GaR) and output, labeled y_t, as endogenous variables. We stack these in the vector $\boldsymbol{x}_t = (\mathrm{ne}_t, y_t)'$ and estimate the following reduced form VAR:

$$\boldsymbol{x}_t = \sum_{l=1}^{P} \boldsymbol{A}_l \boldsymbol{x}_{t-l} + \boldsymbol{B}\boldsymbol{d}_t + \boldsymbol{u}_t, \qquad \boldsymbol{u}_t \sim \mathcal{N}(\boldsymbol{0}, \boldsymbol{\Sigma}), \tag{5}$$

$\boldsymbol{A}_l$ is the dynamic coefficient matrix for lag $l = 1, \ldots, P$, $\boldsymbol{B}$ comprises the parameters associated with deterministic components $\boldsymbol{d}_t = (1, t, t^2)'$ and $\boldsymbol{u}_t = (u_{\mathrm{ne},t}, u_{y,t})'$ are reduced form errors following a multivariate Gaussian distribution with zero mean and covariance matrix $\boldsymbol{\Sigma}$. The structural *belief* (b) and *non-belief* (nb) shocks comprise the vector $\boldsymbol{\epsilon}_t = (\epsilon_{\mathrm{nb},t}, \epsilon_{\mathrm{b},t})'$. They are uncorrelated and their variance is normalized such that $\boldsymbol{\epsilon}_t \sim \mathcal{N}(\boldsymbol{0}, \boldsymbol{I})$. To achieve identification, we need to pin down the elements of the matrix $\boldsymbol{A}_0$, which maps structural shocks to reduced form innovations $\boldsymbol{u}_t = \boldsymbol{A}_0\boldsymbol{\epsilon}_t$. This implies that $\boldsymbol{\Sigma} = \boldsymbol{A}_0\boldsymbol{A}_0'$ and presents a well-known identification problem.

Further restrictions are necessary to give economic meaning to our structural shocks, which we introduce as follows. The belief shock causes a negative co-movement between the nowcast error and

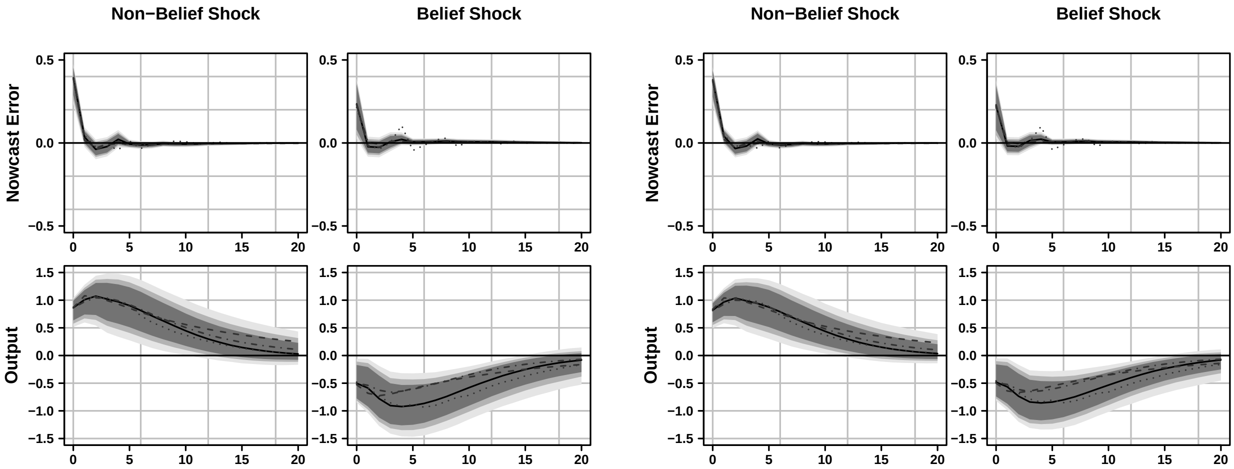

(a) Sample: 1968Q4 – 2014Q4 **(b)** Sample: 1968Q4 – 2019Q4

Fig. 3: Impulse response functions to a non-belief and belief shock.
Notes: Estimation of bivariate Bayesian VAR(4) identified with sign restrictions. Solid black lines are posterior median responses, while gray shaded areas depict the 68/80/90 percent credible sets of the flat prior version of this model. NEs and output are measured in deviations from trend in percentage points. Dashed and dotted lines refer to posterior medians of alternative specifications.

output, because a negative (positive) nowcast error means that the consensus survey expectation of growth is higher (lower) than current output growth in real-time. Hence, agents are overly optimistic which causes an outward (inward) shift of the demand curve and subsequently output increases (decreases). The non-belief shock differs from the belief shock insofar as it causes co-movement between the nowcast error and output. This gives rise to sign restrictions on the elements of $\boldsymbol{A}_0$:

$$\begin{bmatrix} u_{\mathrm{ne},t} \\ u_{y,t} \end{bmatrix} = \begin{bmatrix} + & + \\ + & - \end{bmatrix} \begin{bmatrix} \epsilon_{\mathrm{nb},t} \\ \varepsilon_{\mathrm{b},t} \end{bmatrix},$$

which set-identifies the structural shocks. For estimation and structural inference we rely on Bayesian methods. We use variants of Bayesian VARs with weakly informative Minnesota-type priors, and alternative implementations are noted when applicable. We use a Gibbs sampler and draw 15,000 times from the posterior distribution while discarding the first 5,000 draws as burn-in. For the sign restrictions, we rely on the algorithm proposed by Rubio-Ramirez *et al.* (2010).[5]

3.2. *Revisiting the original belief shocks*

We replicate the main findings of Enders *et al.* (2021) and corroborate their results along several dimensions. First, we consider two sampling periods. Specifically, we apply our framework to the

[5] This algorithm is based on a QR decomposition to draw uniformly from the space of orthonormal matrices to construct $\boldsymbol{A}_0$ that satisfies the sign restriction. The original implementation of Enders *et al.* (2021) uses Givens rotation matrices to draw uniformly from the space of orthonormal matrices. Hence, these approaches draw from the same space of orthonormal matrices to construct $\boldsymbol{A}_0$. An alternative approach that introduces identification information via explicit priors is due to Baumeister and Hamilton (2015).

original sample which ranges from 1968Q4 to 2014Q4, but also use an extended version which runs through 2019Q4.[6] Second, we consider different specifications of the VARs. On the one hand, we vary the number of lags $P \in \{2, 4, 6\}$. On the other hand, we consider both a flat prior (for the "exact" replication of Enders *et al.*, 2021) and the weakly informative prior implementation mentioned above.[7]

Impulse response functions are computed for a horizon of 20 quarters and shown in Figure 3 for the respective subsamples in panels (a) and (b). Non-belief and belief shocks are in the respective left and right columns; the upper rows refer to the NE, while the bottom row depicts the response of output growth. The recovered dynamic responses are virtually identical to those in Enders *et al.* (2021, compare their Figure 5 to our Figure 3(a)), for all considered model specifications. The imposed sign restrictions result in positive co-movement between the NE and output in response to the non-belief shock, and negative co-movement for the belief shock on impact. Note that propagation dynamics are left unconstrained by this identification scheme. The response of the NE is short-lived for both shocks and insignificant for all horizons apart from the impact. The output-response by contrast is fairly persistent. Depending on the level of statistical significance, it turns indistinguishable from zero after about 12 to 15 quarters. A negative NE corresponds to excessively optimistic beliefs. In this case, survey expectations exceed actual real-time output growth, because agents have an optimistic outlook. This optimism about current output growth causes actual output growth to increase.

Varying the number of lags and introducing modest shrinkage via a Minnesota-type prior has minor implications for the persistence of our posterior median estimates. But these differences are statistically insignificant. Comparing the extended sample in Figure 3(b) to the original period in Figure 3(a), as in Enders *et al.* (2021), indicates that this extension has no discernible consequences for the results. To sum up this narrow replication study, we find that the original results are robust to alternative specifications and implementations of the baseline econometric framework.

3.3. *Nowcast errors about growth-at-risk*

In this subsection, we investigate whether nowcast errors about GaR can be used as an alternative reduced form measure to identify belief shocks. These nowcast errors can be interpreted as misjudgments of macroeconomic risk in real-time. The resulting belief shocks potentially differ from the mean-based ones discussed above (e.g., through fundamental macroeconomic or financial shocks asymmetrically affecting the objective versus subjective nowcast distribution of output). The empirical findings of

[6] We thus estimate the model excluding the post-Covid period. Extending the sample further but downweighting/dropping the pandemic observations (see, e.g., Lenza and Primiceri, 2022) yields qualitatively similar results.

[7] Note that Enders *et al.* (2021) carried out their computations in `MATLAB` and relied on a frequentist approach to estimation and inference. By contrast, we have independently compiled the dataset, and use a Bayesian VAR implemented in `R`. This provides robustness from a data, econometric, and software perspective.

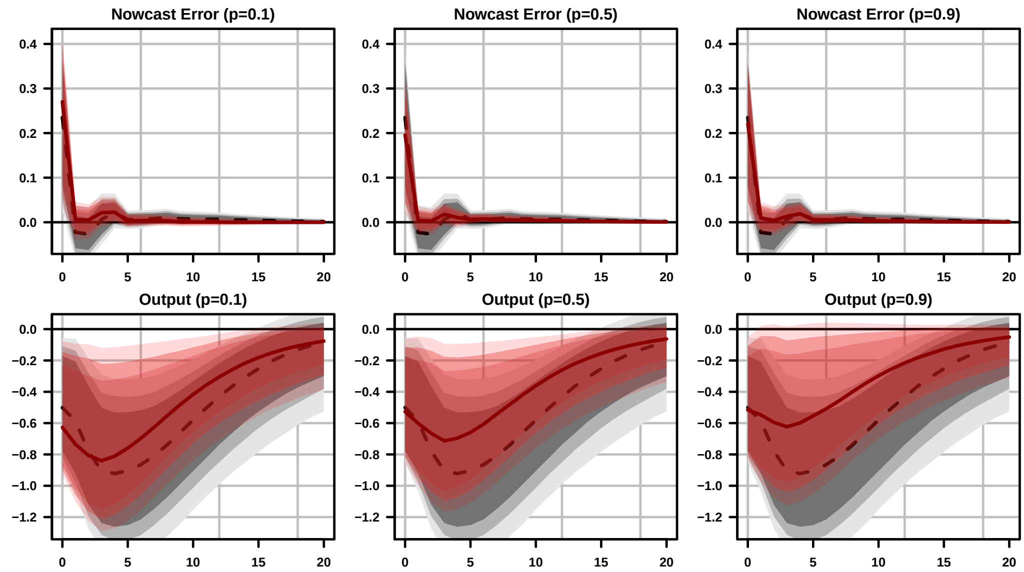

Fig. 4: Impulse response functions to belief shocks using GaR-NEs.

Notes: Estimation of bivariate Bayesian VAR(4) identified with sign restrictions. Black/red lines denote the posterior median responses while gray/red shaded areas depict the 68/80/90 percent credible sets. Nowcast error and output are measured in deviations from trend in percentage points. Responses in black/gray denote the original model of Enders *et al.* (2021), while the responses in red denote the impulse responses to the belief shocks arising from the tails of nowcast distributions.

this section thus also relate to those of Loria *et al.* (2024), who measure quantile-specific responses of output growth to several fundamental (mean-based or externally identified) macroeconomic and financial shocks. By contrast, we use the NEs that originate in the quantiles to pin down shocks in a mean-based linear VAR framework.

Given the robustness of the original results that we established in the preceding section, we limit ourselves to using the full sample ranging from 1968Q4 to 2019Q4, and use a lag length of $P = 4$ in the Bayesian VAR. As pointed out earlier, we now use the full predictive distribution from the SPF and rely on the NEs as defined in Eq. (4) to capture these aspects.[8] The main results from this exercise are presented in Figure 4, in form of the red-colored impulse response functions. The columns now report the dynamic effects of belief shocks for three different quantiles, $p = \{0.1, 0.5, 0.9\}$. Since the nowcast errors are a reduced form measure, we identify belief shocks via sign restrictions using measures of downside, median, and upside risk. For ease of reference, the effects measured in the narrow replication are shown in shades of grey, and the dashed line marks the posterior median estimate from before.

Peak response effects occur slightly earlier and they are also a bit subdued when compared to the original framework. But the credible sets are inflated when considering the quantiles, and the structural VAR yields similar (and statistically indistinguishable) dynamic effects. Overall we thus

[8] The NEs are based on real-time predictions of GaR. In a robustness check, we also estimate the true quantile processes based on full-sample information for the final vintage data of the predictors. The results are robust to this choice.

conclude that considering belief shocks in different parts of the nowcast distribution does not cause any noteworthy differences when the focus is on explaining business cycle fluctuations. The mean-based original implementation is sufficient to induce the characteristic effects which are mostly homogeneous across GaR quantiles. This corroborates the results of Enders *et al.* (2021) in a wide sense. And this finding can, at least in part, be traced back to the notion that SPF nowcasts for output growth in our sampling period are mostly unimodal and symmetric.

But while differences between effects at different probabilities of GaR are statistically insignificant, some interesting heterogeneity still emerges. For instance, zooming into the belief shock using an upside risk NE at $p = 0.9$ we find that the corresponding 90 percent credible set includes zero for all horizons apart from the impact. It is also worth mentioning that the median response is less clearly hump-shaped and flatter, particularly when contrasted with the one for downside risk at $p = 0.1$. This pattern appears monotonically when transitioning from the upper to the lower quantiles (using finer grids of GaR).

We again stress that none of these differences are significant in a statistical sense, but they point towards the notion that the overall effects of belief shocks are at least to some extent driven by misperceptions about adverse economic dynamics (in the lower tails). This is in line with the literature on GaR, which has indeed almost exclusively focused on the lower tails of output growth. Given the linearity of the model, positive and negative shocks yield symmetric effects, so this also implies a somewhat stronger expansion in response to benign belief shocks about downside risk.

4. CLOSING REMARKS

In this paper we replicate the study of belief shocks and their implications by Enders *et al.* (2021). Their results are robust in a narrow sense concerning data sourcing, econometric specification, and software implementation. In a wide sense, we also investigate whether belief shocks differ when using nowcast errors from the tails of the nowcast distribution of output growth. Our findings suggest that the originally proposed approach is sufficient to measure the overall effects of belief shocks on business cycle fluctuations adequately. Distinct patterns in dynamic responses arising from considering the full nowcast distribution are negligible for the most part.

REFERENCES

Adam K, Matveev D, and Nagel S (2021), "Do Survey Expectations of Stock Returns Reflect Risk Adjustments?" *Journal of Monetary Economics* **117**, 723–740.

Adams PA, Adrian T, Boyarchenko N, and Giannone D (2021), "Forecasting Macroeconomic Risks," *International Journal of Forecasting* **37**(3), 1173–1191.

Adrian T, Boyarchenko N, and Giannone D (2019), "Vulnerable Growth," *American Economic Review* **109**(4), 1263–89.

Baumeister C, and Hamilton JD (2015), "Sign Restrictions, Structural Vector Autoregressions, and Useful Prior Information," *Econometrica* **83**(5), 1963–1999.

Beaudry P, and Portier F (2006), "Stock Prices, News, and Economic Fluctuations," *American Economic Review* **96**(4), 1293–1307.

——— (2014), "News-Driven Business Cycles: Insights and Challenges," *Journal of Economic Literature* **52**(4), 993–1074.

Bhandari A, Borovička J, and Ho P (2022), "Survey Data and Subjective Beliefs in Business Cycle Models," *SSRN* **2763942**.

Bianchi F, Ludvigson SC, and Ma S (2022), "Belief Distortions and Macroeconomic Fluctuations," *American Economic Review* **112**(7), 2269–2315.

Boeck M (2023), "Belief Distortions in Risk Premia," SSRN Working Paper No. 4010599.

Born B, Dovern J, and Enders Z (2023), "Expectation Dispersion, Uncertainty, and the Reaction to News," *European Economic Review* **154**, 104440.

Clark TE, Huber F, Koop G, Marcellino M, and Pfarrhofer M (2023), "Tail Forecasting with Multivariate Bayesian Additive Regression Trees," *International Economic Review* **64**(3), 979–1022.

——— (2024), "Investigating Growth-at-Risk Using a Multicountry Nonparametric Quantile Factor Model," *Journal of Business & Economic Statistics* **00**(in-press).

Dovern J, Fritsche U, and Slacalek J (2012), "Disagreement Among Forecasters in G7 Countries," *Review of Economics and Statistics* **94**(4), 1081–1096.

Enders Z, Kleemann M, and Müller GJ (2021), "Growth Expectations, Undue Optimism, and Short-Run Fluctuations," *Review of Economics and Statistics* **103**(5), 905–921.

Frühwirth-Schnatter S (2006), *Finite mixture and Markov switching models*, Springer.

Gneiting T, and Ranjan R (2011), "Comparing density forecasts using threshold-and quantile-weighted scoring rules," *Journal of Business & Economic Statistics* **29**(3), 411–422.

Krüger F, and Nolte I (2016), "Disagreement Versus Uncertainty: Evidence from Distribution Forecasts," *Journal of Banking & Finance* **72**, S172–S186.

Lahiri K, and Sheng X (2010), "Measuring Forecast Uncertainty by Disagreement: The Missing Link," *Journal of Applied Econometrics* **25**(4), 514–538.

Lenza M, and Primiceri GE (2022), "How to Estimate a Vector Autoregression After March 2020," *Journal of Applied Econometrics* **37**(4), 688–699.

Loria F, Matthes C, and Zhang D (2024), "Assessing Macroeconomic Tail Risk," *Economic Journal* **forthcoming**.

Pei G (2024), "Pessimism, Disagreement, and Economic Fluctuations," *Journal of the European Economic Association* **22**(3).

Pfarrhofer M (2022), "Modeling Tail Risks of Inflation Using Unobserved Component Quantile Regressions," *Journal of Economic Dynamics and Control* **143**, 104493.

Rubio-Ramirez JF, Waggoner DF, and Zha T (2010), "Structural Vector Autoregressions: Theory of Identification and Algorithms for Inference," *The Review of Economic Studies* **77**(2), 665–696.

Stock JH, and Watson MW (2002), "Macroeconomic Forecasting Using Diffusion Indexes," *Journal of Business & Economic Statistics* **20**(2), 147–162.

Online Appendix: Belief Shocks and Implications of Expectations about Growth-at-Risk

A. Additional empirical results

To contrast NEs across quantiles and with the original implementation, we complement these time series charts with Figure A1, which shows pairwise scatterplots and a density estimate of the unconditional distribution of the NEs. There is a positive relationship between all considered pairs. In the left panel, we compare the plain NEs with the corresponding central quantile ones at $p = 0.5$. The correlation coefficient ρ is satisfactory for our purposes, with $\rho = 0.83$. In light of the density chart on the right-hand side, this value results at least to some extent from heavier tails when using the actual realizations. Downside risk NEs ($p = 0.1$) are strongly correlated with those for the median at 0.77. Interestingly, while $p = 0.5$ and $p = 0.9$ (upside risk) are also strongly correlated (not shown here), this is not the case for the NEs in each of the tails (rightmost scatterplot), with $\rho = 0.44$.

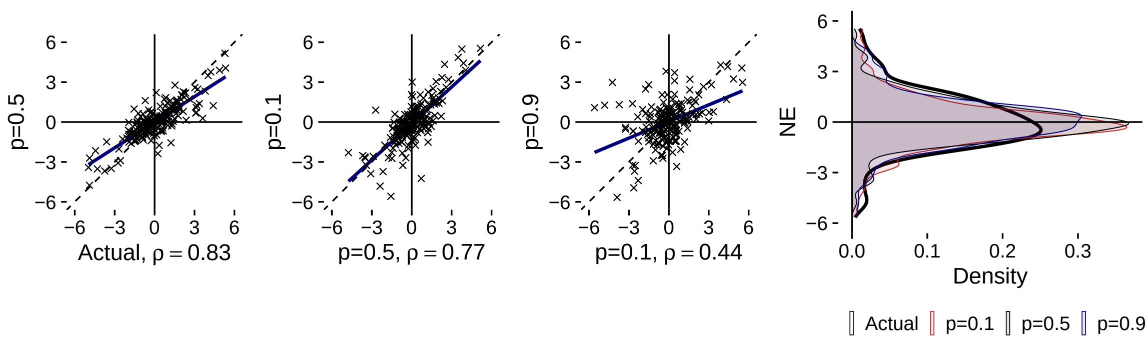

Fig. A1: Scatterplot of NEs computed with actual realizations of real GDP growth and the indicated selected GaR probabilities and density estimates. Grey dashed line indicates 45 degree line while the blue bold line denotes the regression line in the scatterplots and ρ is the correlation coefficient.

B. Real-Time Database

Table B1 lists all variables we use to extract factors; most are taken from the Real-Time Database for Macroeconomists of the Federal Reserve of Philadelphia, and we use first vintages. The dataset starts in 1959Q1. Financial variables (i.e., *Interest Rates*, *Spreads*, *Foreign Exchanges*, and *Stock Markets*) are not revised and taken from FRED-QD. If a series is available monthly, we use the end-of-the-period vintage in each quarter. The column *Tcode* shows transformations: no transformation (1); first difference (2); natural logarithm (4); first difference of natural log (5); second difference in logs (6).

Table B1: Real-Time Macroeconomic Data.

#	Mnemonic	Description	Tcode	Starting Date
Output and Income				
1	ROUTPUT	Real Gross Domestic Product	5	1965Q4
2	NOUTPUT	Nominal Gross Domestic Product	5	1965Q4
3	IPT	Industrial Production Index: Total	5	1962M11
4	IPM	Industrial Production Index: Manufacturing	5	1962M11
5	CUT	Capacity Utilization Rate: Total	1	1983M7
6	CUM	Capacity Utilization Rate: Manufacturing	1	1979M8
7	WSD	Wages and Salary Disbursements	5	1965Q4
8	OLI	Other Labor Income	5	1965Q4
9	PROPI	Proprietor's Income	5	1965Q4
10	RENTI	Rental Income of Persons	2	1965Q4
11	DIV	Dividends	5	1965Q4
12	PINTI	Personal Interest Income	5	1965Q4
13	TRANR	Transfer Payments	5	1965Q4
14	SSCONTRIB	Personal Contribution for Social Insurance	5	1965Q4
15	NPI	Nominal Personal Income	5	1965Q4
16	PTAX	Personal Tax & Nontax Payments	5	1965Q4
17	NDPI	Nominal Disposable Personal Income	5	1965Q4
18	PINTPAID	Interest Paid by Consumers	5	1965Q4
19	TRANPF	Personal Transfer Payments to Foreigners	5	1965Q4
20	NPSAV	Nominal Personal Saving	2	1965Q4
21	RATESAV	Personal Saving Rate, Constructed	2	1965Q4
Consumption and Investment				
22	RCON	Real Personal Consumption Expenditure: Total	5	1965Q4
23	RCONND	Real Personal Consumption Expenditure: Nondurable Goods	5	1965Q4
24	RCOND	Real Personal Consumption Expenditure: Durable Goods	5	1965Q4
25	RCONS	Real Personal Consumption Expenditure: Services	5	1965Q4
26	NCON	Nominal Personal Consumption Expenditure	5	1965Q4
27	RINVRESID	Real Gross Private Domestic Investment: Residential	5	1965Q4
28	RINVCHI	Real Gross Private Domestic Investment: Change in Private Inventories	2	1965Q4
Trade and Government				
29	RNX	Real Net Export of Goods and Services	2	1965Q4
30	REX	Real Exports of Goods and Services	5	1965Q4

Continued on next page

Table B1 – *Continued from previous page*

#	Mnemonic	Description	Tcode	First Vintage
31	RIMP	Real Import of Goods and Services	5	1965Q4
32	RG	Real Government Consumption & Gross Investment: Total	5	1965Q4
33	RGF	Real Government Consumption & Gross Investment: Federal	5	1965Q4
34	RGSL	Real Government Consumption & Gross Investment: State and Local	5	1965Q4
Money and Prices				
35	M1	M1 Money Stock	6	1965Q4
36	M2	M2 Money Stock	6	1971Q2
37	P	Price Index for GNP/GDP	6	1965Q4
38	PCON	Price Index for Personal Consumption Expenditure, Constructed	6	1965Q4
39	PIMP	Price Index for Imports of Goods and Services	6	1965Q4
Labor Market and Housing				
40	RUC	Unemployment Rate	2	1965Q4
41	EMPLOY	Nonfarm Payroll Employment	5	1964M12
42	H	Index of Aggregate Weekly Hours: Total	1	1971M9
43	HG	Index of Aggregate Weekly Hours: Goods Sector	1	1971M9
44	HS	Index of Aggregate Weekly Hours: Service Sector	1	1971M9
45	HSTARTS	Housing Starts	5	1968M2
Interest Rates and Spreads				
46	FEDFUNDS	Effective Federal Funds Rate	1	1959Q1
47	TB3MS	3-Months Treasury Bill: Secondary Market Rate	1	1959Q1
48	TB6MS	6-Months Treasury Bill: Secondary Market Rate	1	1959Q1
49	GS1	1-Year Treasury Constant Maturity Rate	1	1959Q1
50	GS5	5-Year Treasury Constant Maturity Rate	1	1959Q1
51	GS10	10-Year Treasury Constant Maturity Rate	1	1959Q1
52	MORTGAGE30US	30-Year Conventional Mortgage Rate	1	1959Q1
53	AAA	Moody's Seasoned Aaa Corporate Bond Yield	1	1959Q1
54	BAA	Moody's Seasoned Baa Corporate Bond Yield	1	1959Q1
55	BAA10Y	BAA - GS10	1	1959Q1
56	MORTG10YR	BAA - MORTGAGE30US	1	1959Q1
57	TB6M3M	TB6MS - TB3MS	1	1959Q1
58	GS1TB3M	GS1 - TB3MS	1	1959Q1
59	GS10TB3M	GS10 - TB3MS	1	1959Q1
60	CPF3MTB3M	3-Month Commercial Paper Minus 3-Month Treasury Bill	1	1959Q1

Continued on next page

Table B1 – *Continued from previous page*

#	Mnemonic	Description	Tcode	First Vintage
61	TB3SMFFm	TB3MS - FEDFUNDS	1	1959Q1
62	T5YFFM	GS5 - FEDFUNDS	1	1959Q1
63	AAAFFM	AAA - FEDFUNDS	1	1959Q1
64	CP3M	3-Months AA Financial Commercial Paper Rate	1	1959Q1
65	COMPAPFF	3-Month Commercial Paper Minus Federal Funds Rate	1	1959Q1
Foreign Exchange Rates				
66	TWEXMMTH	Trade Weighted U.S. Dollar Index: Major Currencies	5	1959Q1
67	EXUSEU	U.S. / Euro Foreign Exchange Rate (U.S. Dollars to One Euro)	5	1959Q1
68	EXSZUS	Switzerland / U.S. Foreign Exchange Rate	5	1959Q1
69	EXJPUS	Japan / U.S. Foreign Exchange Rate	5	1959Q1
70	EXUSUK	U.S. / U.K. Foreign Exchange Rate	5	1959Q1
71	EXCAUS	Canada / U.S. Foreign Exchange Rate	5	1959Q1
Stock Markets				
72	UMCSENT	University of Michigan: Consumer Sentiment	1	1959Q1
73	USEPUINDXM	Economic Policy Uncertainty Index for United States	2	1959Q1
74	VXOCLS	CBOE S&P100 Volatility Index	1	1959Q1
75	NIKKEI225	Nikkei Stock Average	5	1959Q1
76	NASDAQCOM	NASDAQ Composite Index	5	1959Q1
77	S&P 500	S&P's Common Stock Price Index: Composite	5	1959Q1
78	S&P: indust	S&P's Common Stock Price Index: Industrials	5	1959Q1
79	S&P: div yield	S&P's Common Stock Price Index: Dividend Yield	2	1959Q1
80	S&P PE ratio	S&P's Common Stock Price Index: Price-Earnings Ratio	5	1959Q1